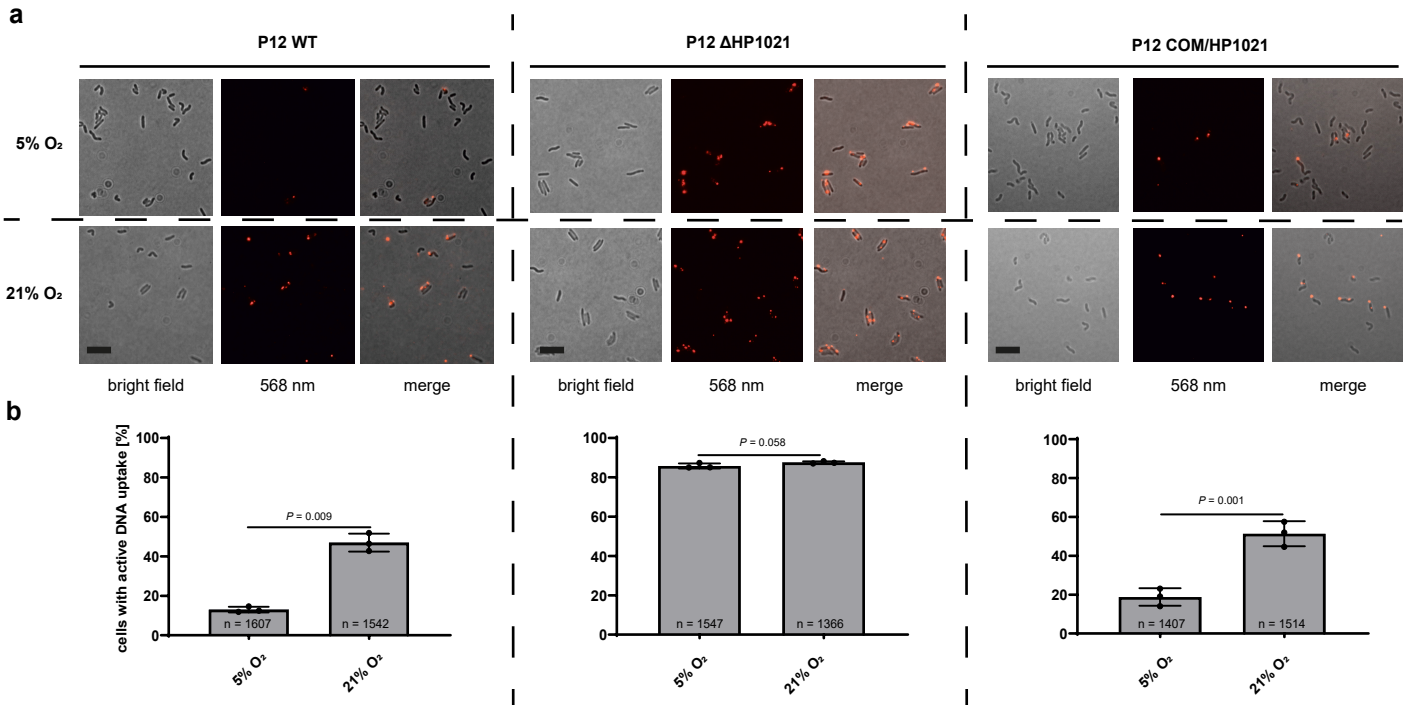

Fig. S9: Analysis of DNA uptake by *H. pylori* P12. a Bright field, fluorescent (532 nm) and merged images of *H. pylori* WT and mutant strains after 15 min of Cy3-λ DNA uptake under microaerobic and aerobic conditions (5% and 21% O_2, respectively). **b** Quantitative analysis of λ-Cy3 DNA foci formation in *H. pylori* under microaerobic and aerobic conditions (5% and 21% O_2, respectively). The scale bar represents 2 µm. Data are depicted as the mean values ± SD. Two-tailed Student's t-test determined the P value. n = number of cells examined over 3 independent biological experiments. Source data are provided with this paper.

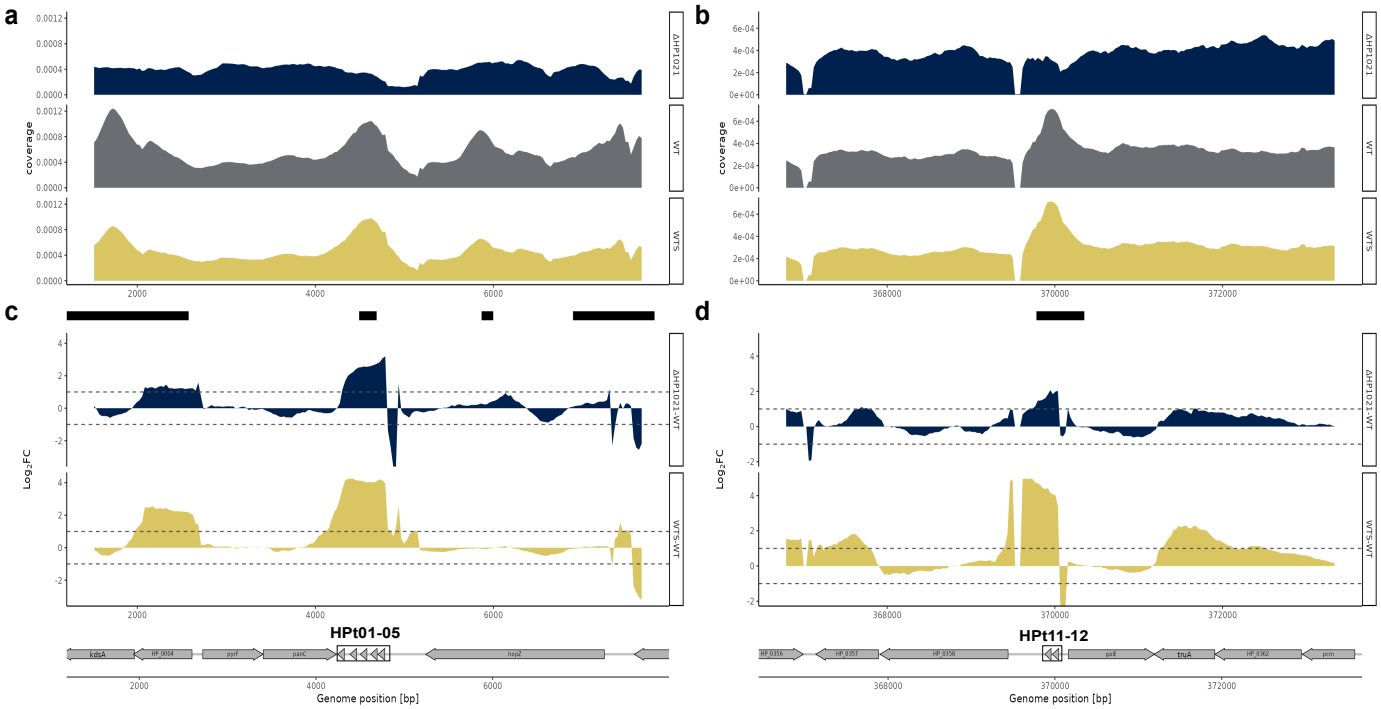

Fig. S10: HP1021 controls tRNA expression. a-b. ChIP-seq data profile of the regions coding tRNAs, namely (a) HPt01-HPt05 and (b) HPt11-HPt12. Read counts were determined for *H. pylori* N6 WT, WTS and ΔHP1021 strains. The y-axis represents the coverage of the DNA reads, while the x-axis represents the position of the genome (in bps). The main peak of the binding site is marked with a thick black line under the x-axis. **c-d** RNA-seq data profile of the regions coding tRNAs, namely (c) HPt01-HPt05 and (d) HPt11-HPt12. The genomic locus for *H. pylori* N6 WT, WTS and ΔHP1021 strains with the WTS-WT and ΔHP1021-WT expression comparison; values above the black dashed lines indicate a change in the expression of $|\log_2 FC| \geq 1$; FDR ≤ 0.05.

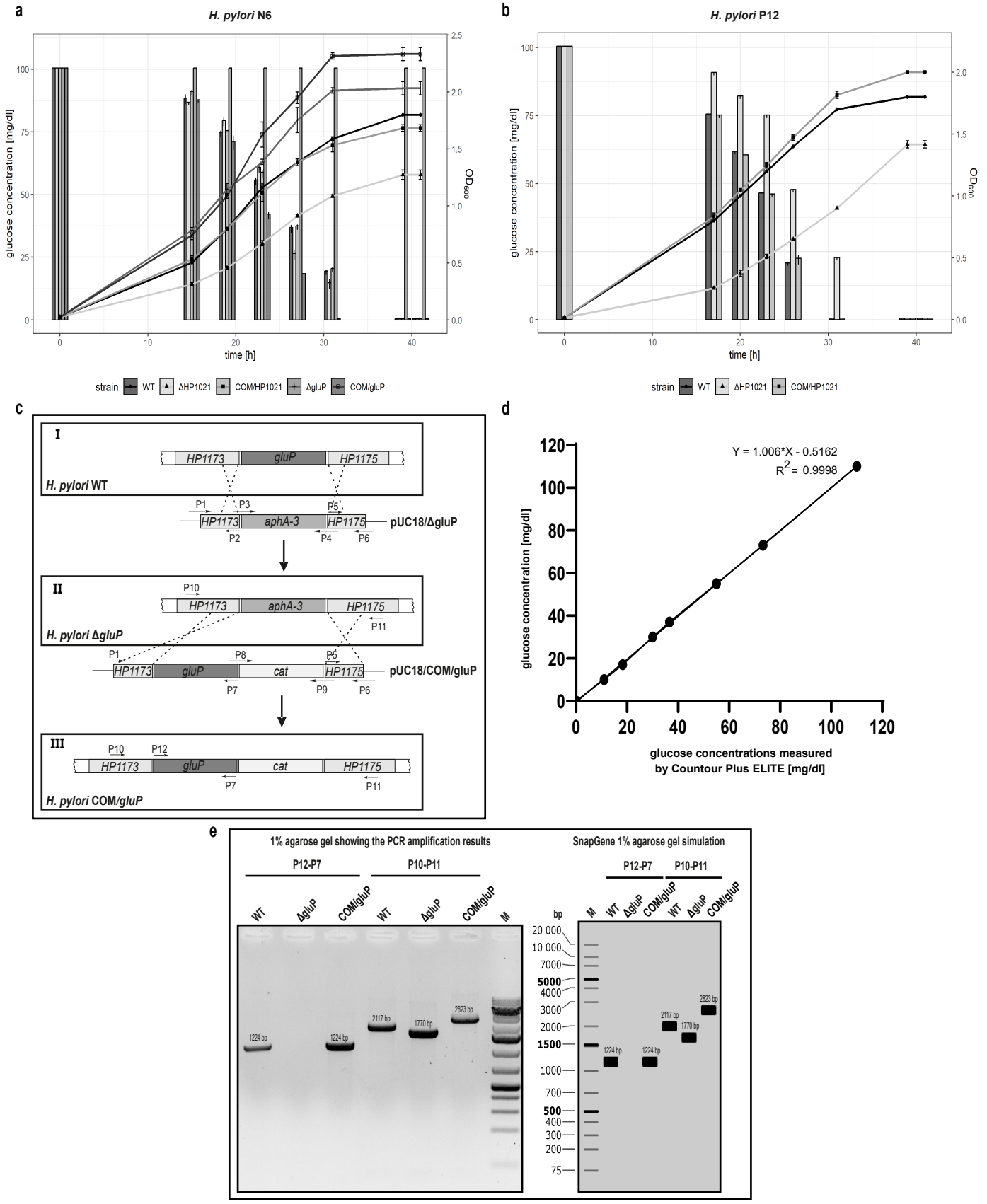

Fig. S11: HP1021 controlled glucose uptake via GluP transporter. a Growth curves of *H. pylori* N6 wild-type and mutant strains (line plot), combined with glucose concentration in the culture (bar plot). **b** Growth curves of *H. pylori* P12 WT, ΔHP1021, COM/HP1021 combined with glucose consumption (bar plot). **c** The mutagenesis strategy used to delete and subsequently complement *gluP* on the *H. pylori* N6 chromosome. *H. pylori* N6 wild-type *gluP* chromosomal loci (I) and plasmid DNA for double crossing-over to give *H. pylori* N6 ΔgluP (II) and COM/gluP (III) mutant strains are shown. For the plasmids and primer sequences, see Supplementary Tables S1 and S2, respectively. **d** Glucose concentration standard curve. The TSBΔD-FBS medium supplemented with glucose (110 mg/dl) was serially diluted with 1 × PBS, and the glucose concentration of the appropriate dilutions was measured with Contour Plus ELITE. **e** Agarose gel electrophoresis of PCR products confirming the correct *H. pylori* N6 ΔgluP and COM/gluP mutant strain construction with SnapGene® agarose gel simulation. M, GeneRuler™ 1 kb Plus DNA Ladder (Thermo Fisher Scientific). The experiment was repeated once. **a-b** n = 3 biologically independent experiments. Source data are provided with this paper.

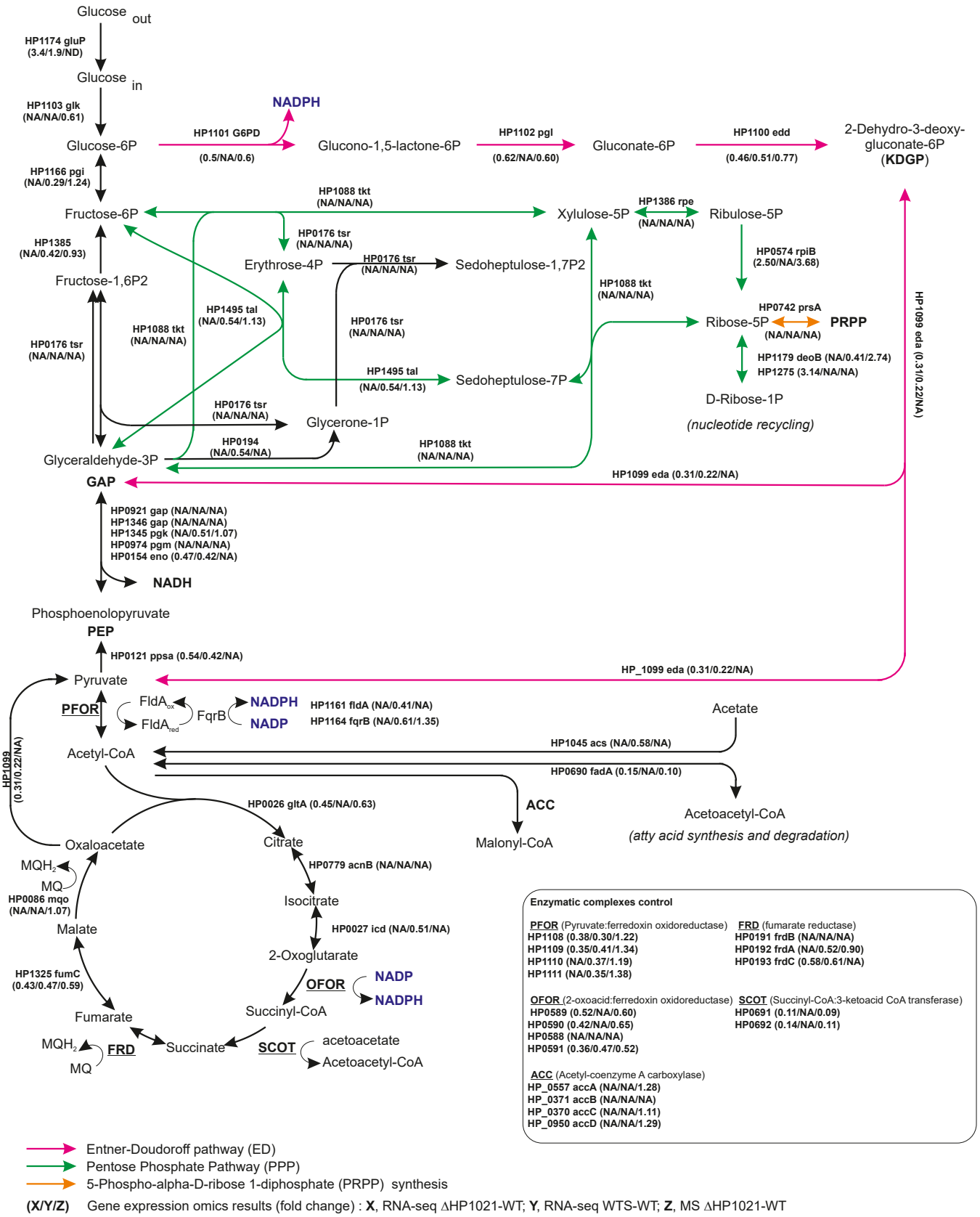

Fig. S12: A model of glucose metabolism in *H. pylori* N6 based on KEGG database and Steiner et al.[7]. Genes annotation according to *H. pylori* 26695 (NC_000915.1) strain . MQ, menaquinone; Fd, ferredoxin; NA, indifferent gene (the change was not significant); ND, not detected.

Supplementary References

1. Sambrook, J. & Russel, D. W. *Molecular Cloning: A Laboratory Manual*. *Cold Spring Harbor Laboratory Press* Cold Spring Harbor Laboratory Press, New York (2001).
2. Tomb, J. F. *et al.* The complete genome sequence of the gastric pathogen *Helicobacter pylori*. *Nature* **388**, 539–547 (1997).
3. Ferrero, R. L., Cussac, V., Courcoux, P. & Labigne, A. Construction of isogenic urease-negative mutants of *Helicobacter pylori* by allelic exchange. *J. Bacteriol.* **174**, 4212–4217 (1992).
4. Szczepanowski, P. *et al.* HP1021 is a redox switch protein identified in *Helicobacter pylori*. *Nucleic Acids Res.* **49**, 6863–6879 (2021).
5. Donczew, R. *et al.* The atypical response regulator HP1021 controls formation of the *Helicobacter pylori* replication initiation complex. *Mol. Microbiol.* **95**, 297–312 (2015).
6. Donczew, R., Weigel, C., Lurz, R., Zakrzewska-Czerwińska, J. & Zawilak-Pawlik, A. *Helicobacter pylori oriC* — the first bipartite origin of chromosome replication in Gram-negative bacteria. *Nucleic Acids Res.* **40**, 9647 (2012).
7. Steiner, T. M. *et al.* Substrate usage determines carbon flux via the citrate cycle in *Helicobacter pylori*. *Mol. Microbiol.* **116**, 841–860 (2021).

Description of Additional Supplementary Files

Supplementary Data 1:
Identification of HP1021 binding sites on *H. pylori* N6 genome by ChIP-seq. Chromosome position defined according to *H. pylori* 26695 strain (NC_000915.1).

Supplementary Data 2:
Analysis of HP1021 dependent gene expression in *H. pylori* N6 WT and ΔHP0121 strains under microaerobic and aerobic conditions. RNA-seq, ChIP-seq and LC-MS/MS data are presented. Genes annotation according to *H. pylori* 26695 strain (NC_000915.1).

Supplementary Data 3:
Comprehensive ChIP-seq, RNA-seq and MS data results for genes of selected processes or pathways in *H. pylori* N6. Genes annotation according to *H. pylori* 26695 strain (NC_000915.1). ComB uptake system according to Fisher et al., 2020 and Damke et al., 2022. The glucose metabolism pathway is based on the KEGG database, Kather at al. 2000, Corthesy-Theulaz et al. 1997 and Steiner et al. 2021. ROS and RNS response according to Flint et. al 2016. Transcriptomic and proteomic data are presented as $\log_2$-fold changes. Legends specific to each pathway/process were added below particular tables. For more data, see Supplementary Data 1.

The Additional Supplementary Files are available in open access under the link https://www.nature.com/articles/s41467-023-42364-6#additional-information and on the CD (Appendix) attached to the dissertation.